Soft Matter

PAPER

View Article Online
View Journal

Cite this: DOI: 10.1039/c4sm01625d

Magneto-optic and converse magnetoelectric effects in a ferromagnetic liquid crystal

Alenka Mertelj,*[a] Natan Osterman,[a] Darja Lisjak[a] and Martin Čopič[ab]

We have studied the response of ferromagnetic liquid crystals to external magnetic and electric fields, and compared it to the usual response of nematic liquid crystals (NLCs). We have observed effects, which are not present in a pure NLC and are a consequence of the coupling between the nematic director and the magnetization. The electro-optic effect, which is in the ferromagnetic phase the same as in the pure NLC, is accompanied by a converse magnetoelectric effect. The magneto-optic effect differs completely from the one observed in the pure NLC, where it is a quadratic effect and it only appears when a magnetic field larger than a critical field is applied perpendicular to the director. In the ferromagnetic NLC in addition to the response to the perpendicular field, there is also a qualitatively different response to the parallel field. Contrary to the pure NLC no critical field needs to be exceeded for the system to respond to a perpendicular field, but a critical field needs to be exceeded to observe a response to the field parallel to the director and antiparallel to the magnetization. The critical field is in this case two orders of magnitude smaller than the critical field of the magnetic Frederiks transition in the pure NLC. The experimental observations are well described by a simple macroscopic theory.

Received 23rd July 2014
Accepted 28th August 2014

DOI: 10.1039/c4sm01625d

www.rsc.org/softmatter

Introduction

In solid materials polar ordering, *i.e.*, ferromagnetic or ferroelectric ordering, has been known for a long time and is still widely studied due to its importance in many applications. The crucial constituents of materials that exhibit polar phases are magnetic or electric dipoles. If the interaction between the dipoles is large enough, they orient in the same direction which results in macroscopic spontaneous magnetization $\mathbf{M}$ or electric polarization $\mathbf{P}$, which are the order parameters of polar phases. Long range polar ordering in liquids is rare. Ferromagnetic liquid phases have been observed in liquid helium,[1] undercooled liquid metal alloys,[2] and recently, in suspensions of ferromagnetic platelets in a nematic liquid crystal (NLC).[3] Ferroelectric order appears in the ferroelectric liquid-crystal layered phases made of chiral rodlike molecules[4] or polar bent core molecules,[5] and also in some columnar phases.[6,7]

The most important property of polar materials is their strong response to external fields. Even more interesting are materials that possess two order parameters, which are sensitive to different external fields. Such materials are called multiferroics and are subjects of many studies.[8–12] If such a material possesses simultaneously magnetization and electric polarization and if the two order parameters are coupled, electric polarization is not only affected by an electric field but also by a magnetic field. The effect is called direct magnetoelectric effect, while the opposite effect, *i.e.*, when the magnetization is controlled by a electric field, is called the converse magnetoelectric effect. These effects have been observed in many solid materials.[9–11]

The discovery of ferromagnetic ordering in suspensions of ferromagnetic platelets in NLCs gives us a unique opportunity to study similar effects in a liquid. In these suspensions polar magnetic ordering is accompanied by orientational ordering of NLC.

In NLCs elongated molecules on average orient along a common direction, called the director, which is usually denoted by a unit vector $\mathbf{n}$ with inversion symmetry $\mathbf{n} \equiv -\mathbf{n}$. The nematic phase is not polar, and the order parameter of the phase is a traceless tensor $\underline{\mathbf{Q}} = S\left(\mathbf{n}\otimes\mathbf{n} - \frac{1}{3}\underline{\mathbf{I}}\right)$, where S is the scalar order parameter describing how well the molecules are on average oriented along $\mathbf{n}$.[13] At a constant temperature (and away from defects) S is constant, and the nematic order can be described only by $\mathbf{n}$.

Orientation of $\mathbf{n}$ is affected by external fields. While the terms in the free energy density describing coupling of a polar order with external fields are linear in the field, *e.g.* $-\mu_0\mathbf{M}\cdot\mathbf{H}$ or $-\mathbf{P}\cdot\mathbf{E}$, the terms describing the coupling of the nematic order with an external field are quadratic,[14] $-\varepsilon_a\varepsilon_0(\mathbf{E}\cdot\underline{\mathbf{Q}}\cdot\mathbf{E})$ or $-\chi_a\mu_0(\mathbf{H}\cdot\underline{\mathbf{Q}}\cdot\mathbf{H})$, where μ_0 is the vacuum permeability and ε_0 is the vacuum permittivity. The dielectric anisotropy ε_a and the magnetic anisotropy χ_a are the differences of dielectric constant

[a]J. Stefan Institute, P.O.B. 3000, SI-1001 Ljubljana, Slovenia. E-mail: alenka.mertelj@ijs.si; Fax: +386 1477 3998; Tel: +386 1477 3283
[b]Department of Physics, Faculty of Mathematics and Physics, University of Ljubljana, Jadranska cesta 19, SI-1000 Ljubljana, Slovenia

and magnetic susceptibility along and perpendicular to **n**, respectively. If the anisotropy is positive, **n** tends to align along the corresponding external field.

The NLCs are also birefringent with the optical axis parallel to **n**. In the usual electro-optic and magneto-optic effects the external field changes the orientation of **n**, which consequently affects the propagation of polarized light through the sample. While the magnetic anisotropy is small and usual NLCs do not respond to small magnetic fields, the dielectric anisotropy is large ($\varepsilon_a \approx 10$) and consequently a strong electro-optic response forms the basis for the ubiquitous presence of modern liquid-crystal displays.

Similar to magnetoelectric materials, which are described by coupled **M** and **P**, a suspension of ferromagnetic nanoplatelets in a NLC can be macroscopically described by coupled **M** and **n**, where **M** describes the density of magnetic moments. The coupling is a result of the interaction of the NLC with the surface of the nanoplatelets, which is in our case such that in the absence of an external field the order parameters are parallel. **M** directly responds to magnetic fields and **n** to electric fields. However, due to their coupling **M** also indirectly responds to the electric field and, *vice versa*, **n** to the magnetic field. These are converse magnetoelectric and (indirect) magneto-optic effects, respectively.

Like the electro-optic effect these effects in NLCs differ from the analogous ones in solid materials. The reorientation of **M** in solids happens by the reorientation of magnetic moments (spins), while the crystal orientation remains the same. In a ferromagnetic NLC the reorientation of **n** and **M** is the reorientation of the molecules and platelets, *i.e.*, "the crystal", and is consequently also accompanied by a flow of the material. This leads to the characteristic continuous variation of order parameters and a complex dynamic response of the system. Here we focus on static properties.

Theory and results

In the studied suspension of magnetic nanoplatelets in the NLC the surface of the nanoplatelets was treated so that they orient with their short axis parallel to **n**. Magnetic interaction between the platelets was such that the magnetic moments of the particles were aligned ferromagnetically, which resulted in a macroscopic **M** along **n** (Fig. 1).[3]

We used typical NLC cells in which a liquid crystal is placed between two glass plates with surfaces treated so that in the absence of external fields **n** and **M** were homogeneously oriented in the plane of the cell (Fig. 1a). If an external field is applied perpendicular to **n**, both order parameters vary continuously with the position, so that (at constant temperature, pressure, **H**, and the electric displacement field **D**) the total free energy,

$$F = F_0 + F_{\text{elast}} + F_{\text{coupl}} + F_{\text{D,H}} + F_{\text{surf}}, \quad (1)$$

is minimal. F_0 is the free energy describing the ferromagnetic nematic phase. It includes only the magnitude of **M** and the scalar order parameter of the nematic phase S, which are at

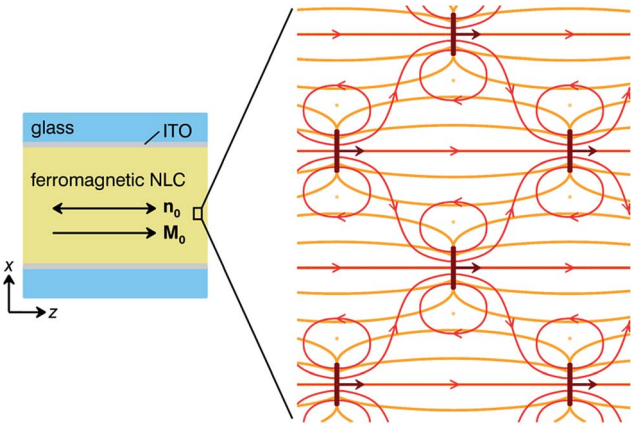

Fig. 1 A schematic of a LC cell (left) and the microscopic structure of the ferromagnetic suspension (right). Glass plates (blue) have ITO electrodes (gray). In the absence of an external field the average macroscopic director $\mathbf{n_0}$ and magnetization $\mathbf{M_0}$ are homogeneously oriented in the plane of the cell. Microscopically the director (orange) is distorted around the platelets (dark red, represented side-on). Dark red arrows indicate magnetic moments and a red line magnetic field.

constant temperature assumed to be constant. If **n** varies with position, there is an additional Frank elastic energy:[13]

$$F_{\text{elast}} = \frac{1}{2}\int_0^d \Big(K_1(\nabla\cdot\mathbf{n})^2 + K_2(\mathbf{n}\cdot(\nabla\times\mathbf{n}))^2 + K_3(\mathbf{n}\times(\nabla\times\mathbf{n}))^2\Big)\mathrm{d}x, \quad (2)$$

where K_i (i = 1, 2, 3) are the splay, twist and bend elastic constants, respectively. There are similar elastic terms associated with the deformation of **M**. They are identical to the nematic elastic terms, where we replace **n** with **M** and K_i with the so called spin-wave stiffness constants A_i. We have estimated A_i to be at least two orders of magnitudes smaller than K_i and neglected these terms.[15] The coupling term[3]

$$F_{\text{coupl}} = -\frac{1}{2}\int_0^d \gamma\mu_0(\mathbf{n}\cdot\mathbf{M})^2\mathrm{d}x \quad (3)$$

describes the coupling between the order parameters, where γ is the coupling constant, and

$$F_{\text{D,H}} = \int_0^d \Big(-\mu_0\mathbf{M}\cdot\mathbf{H} + \frac{1}{2}\mathbf{D}\cdot\mathbf{E}\Big)\mathrm{d}x \quad (4)$$

is the coupling of **M** and **n** with external fields. Here $\varepsilon_0\mathbf{E} = \underline{\boldsymbol{\varepsilon}}^{-1}\mathbf{D}$ and the dielectric tensor $\underline{\boldsymbol{\varepsilon}} = \varepsilon_\perp\underline{\mathbf{I}} + \varepsilon_a\mathbf{n}\otimes\mathbf{n}$, where $\varepsilon_\perp$ is the dielectric constant perpendicular to the director. Because the magnetic anisotropy is small, we neglected the direct coupling of **n** with **H**.

In the surface term,[13]

$$F_{\text{surf}} = -\frac{1}{2}W(\mathbf{n}\cdot\mathbf{n}_s)^2, \quad (5)$$

W is the strength of the surface anchoring and $\mathbf{n}_s$ is the preferred direction of **n** at the surface.

We assume that the physical quantities depend only on coordinate x (Fig. 1), so only the integration over the thickness of the cell d is needed.

Response to the electric field

Firstly, we looked at the response of the system to an external electric field. We measured the changes in the orientation of **M** and **n** as a function of the amplitude of the AC voltage U_{amp} applied between the glass plates. Reorientation of **n** was determined by measuring the phase difference between ordinary and extraordinary light (see experimental methods). For evaluation of the reorientation of **M** its component along the applied field was measured.

The response of **n** was typical of the NLC in an external field (Fig. 2b), *i.e.*, **n** remained unchanged until a critical voltage was exceeded, then it underwent the so-called Frederiks transition to a deformed state (Fig. 2a). Such behavior is a result of the competition between the elastic energy, which is zero in the undeformed state, and the electric energy, which is the smallest when **n** is parallel to the external field. The orientation of **n** at the surface is determined by the boundary conditions, which prevent a homogeneous reorientation of **n** along the external field. The critical voltage U_c at which Frederiks transition occurs is determined by the splay elastic constant K_1, the dielectric anisotropy ε_a, and the surface anchoring W. The sharpness of the transition depends on the angle that $\mathbf{n}_s$ forms with the surface (pretilt). Frederiks transition thus enables measurements of K_1, ε_a, W, $\mathbf{n}_s$ and also K_3, which influences the deformation of **n** above U_c.

The magnetization **M** behaved similarly (Fig. 2c). Its component along the electric field started to increase at the critical voltage and then saturated at the same voltage as the phase difference. In this case the distortion of **M** followed the distortion of **n**, since no additional torque was acting on it, *i.e.*, no external magnetic field or boundary conditions.

We calculated the distortion of **n** and **M** under the external voltage by numerical minimization of the free energy (eqn (1)) and determined the parameters that describe the experiments best using a least square fitting procedure (see experimental methods). Fits are shown as lines in Fig. 2b and c. For comparison, Frederiks transition of the pure NLC is also shown. From the measurements of the phase dependence on the external voltage also the anisotropy of the index of refraction Δn can be determined. We compared Δn and the elastic constants K_1 and K_3 in the suspensions with the measured in the pure NLC: $\frac{\Delta n}{\Delta n_{pure}} = 0.96$, $\frac{K_1}{K_{1,pure}} = 0.89$, and $\frac{K_3}{K_{3,pure}} = 0.92$. The anisotropy Δn is proportional to the nematic scalar order parameter S and the elastic constants are roughly proportional to S^2.[13] The decrease of K_3 in the suspension corresponds to the decrease of S, determined from Δn, while the decrease of K_1 is slightly larger. The obtained anchoring strength and the pretilt angle are $W = (3.4 \pm 0.11) \times 10^{-5}$ J m^{-2} and $\varphi_s = 0.03 \pm 0.01$ rad for 5CB, and $W = (4.3 \pm 0.11) \times 10^{-5}$ J m^{-2} and $\varphi_s = 0.15 \pm 0.022$ rad for the suspension. The values for anchoring strength are typical and the pretilt angle for 5CB is in the range specified by the cell producer. In the case of the suspension the transition is less sharp and that gives an apparent pretilt angle larger than for 5CB.

Response to the magnetic field

Next, we studied the response to a small external magnetic field applied perpendicularly to **n** and **M**. In pure NLCs, analogously to electric transition, magnetic Frederiks transition can be observed as a result of the direct coupling of **n** with **H**.[13] The critical field needed to reorient **n** in the magnetic case depends on K_1 and the magnetic anisotropy χ_a, which is small, *e.g.*, for the NLC we used, $\chi_a = 1.6 \times 10^{-6}$. That gives the critical magnetic field of 290 mT for the LC cell thickness used in our experiments. The magnetic fields we applied were smaller than 20 mT, so the pure NLC remained undistorted.

The situation was different in the case of the ferromagnetic suspension. Most significantly, no critical field was needed to induce the distortion of **n** and **M** (Fig. 3), which is characteristic polar behavior. The component of the magnetization in the field direction initially increased linearly with the external field and saturated in the fields higher than 10 mT. No hysteresis was observed.

In this case the torque of the external magnetic field acts on **M** to reorient it perpendicularly to the initial direction, while the torque at the LC cell surface and the nematic elastic torque act on **n** to keep it in the initial direction. If no coupling of **n** to **M** existed, **M** would align along the field and **n** would remain undisturbed. For a finite coupling the deformation of **n** is smaller than that of **M** as depicted in Fig. 3a.

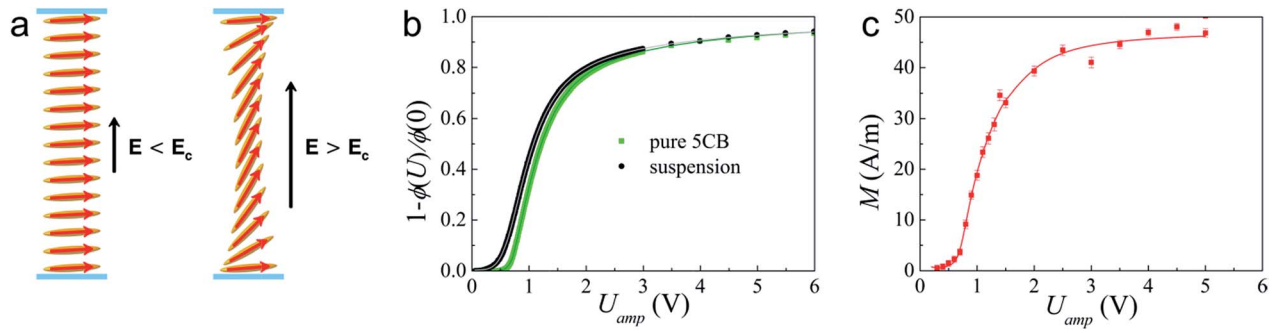

Fig. 2 Electro-optic and converse magnetoelectric effects. (a) A schematic of the director orientation **n** (orange ellipsoids) and the magnetization **M** (red arrows) below and above the critical electric field. (b) Normalized phase difference *vs.* applied voltage showing an electro-optic response. (c) Magnetization *vs.* applied voltage showing a converse magnetoelectric effect. The error bars indicate SEM. Lines are the fits (see text).

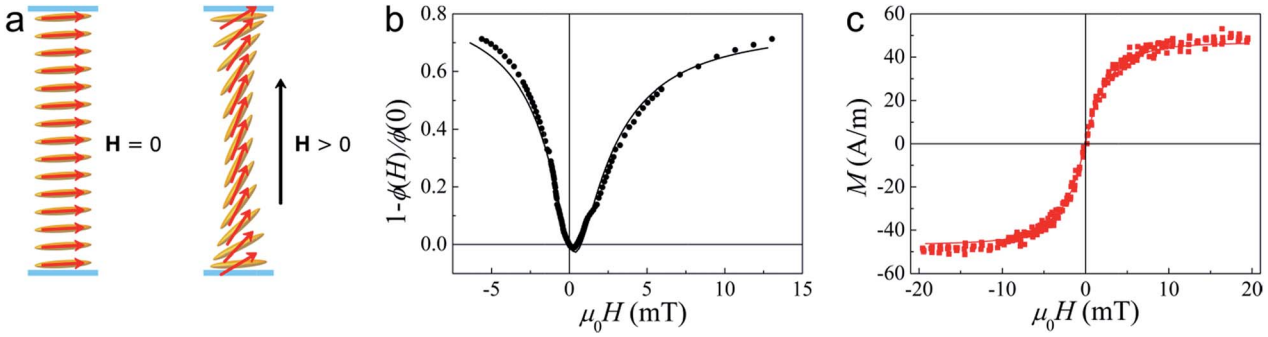

Fig. 3 Magneto-optic effect in a transverse field. (a) A schematic of the director orientation **n** (orange ellipsoids) and the magnetization **M** (red arrows) with and without a magnetic field. (b) Normalized phase difference *vs.* external magnetic field showing a magneto-optic response. Pure 5CB remains undisturbed at these fields. (c) Magnetization curve. Induced magnetization of pure 5CB is less than 0.1 A m^{-1} at these fields. Lines are the fits (see text).

Again we fit the results as described for the electric case. Because the dependency between the elastic constants and the coupling parameter γ in the fitting procedure is significant, we fixed the elastic constants to the values obtained in the electric measurements. The dependence of **M** on **H** gives $\gamma = 110 \pm 70$ and from the fit of the phase dependence we obtain $\gamma = 60$. The fit of the latter describes the behavior qualitatively well, however, the measured phase difference $\phi(H)$ at larger H is smaller than expected. This is probably the result of increasing light scattering with an increasing magnetic field which was observed in the experiments. The scattering is due to larger deformations of the director around the platelets, which also cause a decrease of $\phi(H)$. The minimum of $1 - \frac{\phi(H)}{\phi(0)}$ is shifted to positive values because of a finite pretilt of $\mathbf{n}_s$. The dependence of the response on the thickness d of the cell is different from the usual magnetic Fredericks transition, where the critical field scales as $1/d$. For strong anchoring, *i.e.*, $K/W \ll d$, the field needed to induce a typical distortion in a ferromagnetic NLC scales as $1/d^2$. For weak anchoring, $K/W \approx d$, this field also depends nonanalytically on W.

If an external field is applied along **n** in a NLC with a positive ε_a (or χ_a in the case of magnetic field), orientation of **n** will not be affected. A ferromagnetic NLC, however, is polar and thus sensitive also to the sign of the external magnetic field. If the magnetic field is applied in the direction of **M**, both **M** and **n** remain undistorted. On the other hand, when it is applied in the opposite direction of **M**, it is energetically favorable for **M** to reverse. Indeed a reversal of **M** and **n** is observed when a small critical field $\mathbf{H}_c$ is exceeded (Fig. 4b and c). There is a difference between this case and the case when the field is applied perpendicularly to **M**, where no critical field is observed. The magnetic torque $\mu_0\mathbf{M} \times \mathbf{H}$ is for $\mathbf{H} \perp \mathbf{M}$ maximal, while for $-\mathbf{H} \| \mathbf{M}$ it is zero. In the latter case the system is in a metastable state and any distortion of **n** and **M** is driven by thermal fluctuations. So to understand the difference and why there is a critical field in one case and not in the other, we have to look at these fundamental hydrodynamic excitations of **n** and **M**. In the equilibrium due to thermal excitations the orientation of **n** and **M** fluctuates around the average orientation $\mathbf{n_0}$ and $\mathbf{M_0}$ (Fig. 5a). The eigenmodes of fluctuations are overdamped waves with amplitudes and relaxation times that depend on the wavevector **q** and viscoelastic properties of the material.[13] The slowest, fundamental eigenmode has the largest amplitude and is the one with the smallest wavevector. In a finite sample the smallest wavevector is given by $q_0 \approx \frac{\pi}{d}$, where d is the sample size. In a NLC slab there are two fundamental modes, *i.e.* the splay and the twist (Fig. 5a and b).

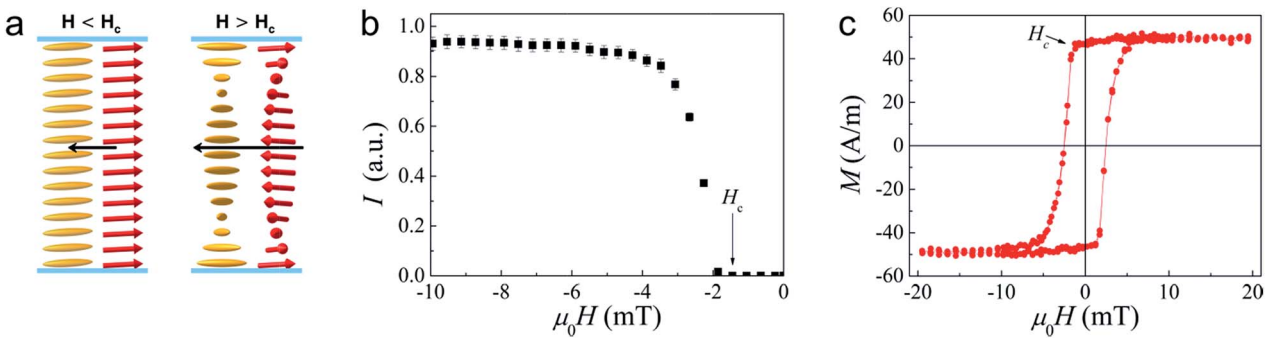

Fig. 4 Magneto-optic effect in a parallel field. (a) A schematic of the director orientation **n** (orange ellipsoids) and the magnetization **M** (red arrows) below and above the critical magnetic field. (b) Transmitted light intensity through the sample between crossed polarizers as measured by polarizing microscopy. Error bars indicate SEM. (c) Magnetization curve.

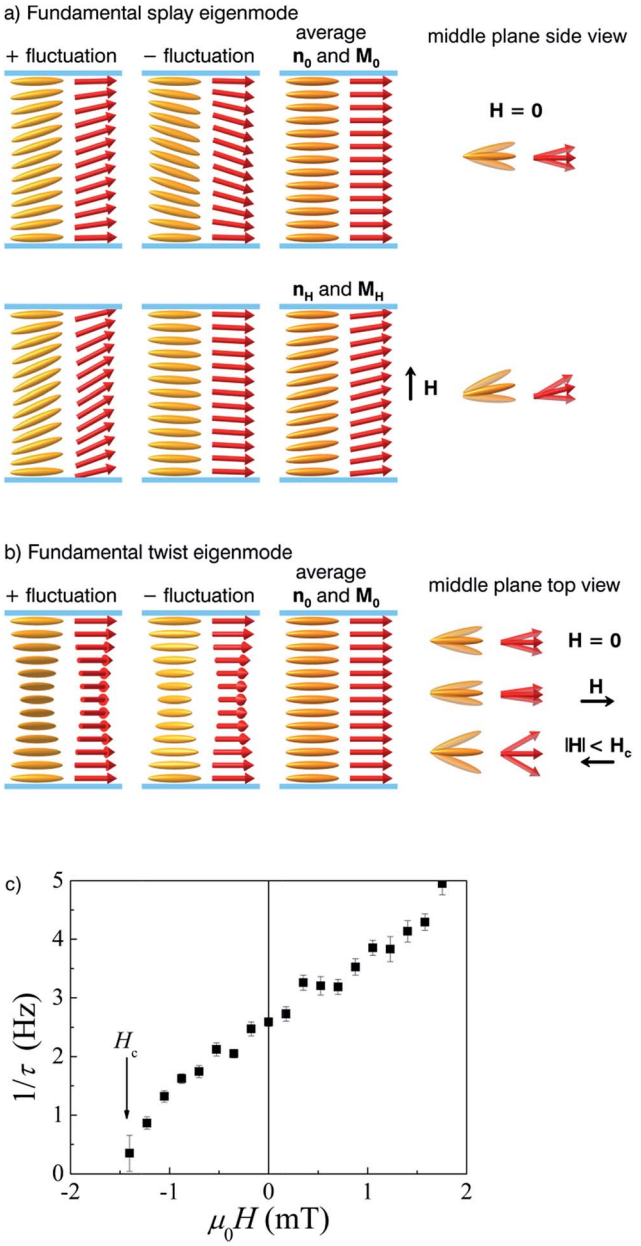

Fig. 5 Fundamental eigenmodes of thermal orientational fluctuations in a slab of a ferromagnetic liquid crystal. (a) Comparison of the fundamental splay eigenmode in a zero field and in a small magnetic field showing a transverse magneto-optic response. (b) The twist fluctuations below the critical magnetic field. (c) Relaxation rate of twist fluctuations *vs.* a parallel external magnetic field showing slowing down of the fluctuations when approaching the critical field. Error bars indicate 1σ uncertainty of the least square fits.

When an eigenmode is thermally excited, there is a distortion of **n** and **M**, and, consequently, an elastic torque that drives relaxation of **n** and **M** back to $\mathbf{n_0}$ and $\mathbf{M_0}$. A viscous torque opposes this relaxation. When an external magnetic field is applied, there is an additional torque that changes the relaxation times and amplitudes of fluctuations. When the field is applied in the direction of $\mathbf{M_0}$, this torque will add to the elastic one and make the relaxation of fluctuations faster and their amplitudes smaller (Fig. 5b). If the magnetic field is applied perpendicular to $\mathbf{M_0}$, the additional torque will increase the amplitude of the fluctuations with amplitudes towards the field direction and will decrease the fluctuations away from it. Larger fluctuations will also be slower. As a consequence the average directions $\mathbf{n_H}$ and $\mathbf{M_H}$ will be tilted towards the field and distorted (Fig. 5a). When a field is applied in the opposite direction to $\mathbf{M_0}$, the field will slow down all fluctuations equally and they will have the same larger amplitude. As long as the elastic torque is larger than the field one, **n** and **M** will relax back to $\mathbf{n_0}$ and $\mathbf{M_0}$ (Fig. 5b). When the field is increased the fluctuations become larger and slower. At the critical field both the amplitude and relaxation times of the fundamental eigenmode diverge and the torque, which drives this relaxation to the equilibrium, is zero. Consequently, when this eigenmode is thermally excited, **n** and **M** do not relax back, but remain in a distorted state, which is now a new equilibrium state. A similar argument explains the critical field of the usual Frederiks transition[13,16] and the experiments showing critical slowing down of fluctuations in the usual NLCs at electric,[17] magnetic,[18] and optic[19] Frederiks transitions have been performed using different light scattering techniques.

In the ferromagnetic NLC we have measured critical slowing down of the fluctuation using differential dynamic microscopy[20,21] (experimental methods). Fig. 5c shows the dependence of the measured relaxation rate $\frac{1}{\tau}$ of the fluctuations on the external magnetic field. It goes to zero approximately at the same critical field as magnetization reversal starts (Fig. 4b). This critical field has been shown to be[3]

$$H_c = -\frac{\gamma M K_2 \pi^2}{K_2 \pi^2 + \gamma \mu_0 M^2 d^2} \tag{6}$$

The reversal of magnetization starts as a twist deformation, so the relevant elastic constant is K_2. From the values for $M = 47$ A m^{-1}, $K_2 = 3.5$ pN, and $\mu_0 H_c = 1.5$ mT we get $\gamma = 130$, which is in agreement with the values obtained from the fits.

Coupling coefficient and anchoring

The value of the coupling coefficient can be estimated from the microscopic picture. Let us assume a very thin platelet with the surface S_0, thickness d_{pl} and anchoring strength W_{pl}. The total surface energy of a single platelet is $2S_0F_{surf}^{platelet} = -S_0W_{pl}(\mathbf{n}\cdot\mathbf{m}_s)^2$. Here $\mathbf{m}_s$ is the preferred direction of the director on the particle surface, *i.e.*, in our case of perpendicular anchoring it is parallel to **M**. If the platelets were independent, the corresponding coupling energy density is obtained by multiplying this energy by number density:

$$F_{coupl} \approx -\int_0^d \frac{cW_{pl}}{d_{pl}}(\mathbf{n}\cdot\mathbf{m}_s)^2 dx \tag{7}$$

This can be compared to eqn (3). c is the volume fraction. A similar expression for cylindrical particles was derived in (ref. 22). From the measured coupling coefficient γ, we can get an

estimate for $W_{pl} \approx 3 \times 10^{-6}$ J m^{-2}. The estimated anchoring of the director at the platelets surface is rather weak. However, this is only a crude estimate giving the upper value of the anchoring, since the platelets are not independent, *i.e.*, they interact elastically, due to nematic mediated interaction, and magnetically. They are also polydisperse.

Comparison with paramagnetic suspensions

Since **n** is coupled to the surface of magnetic particles, ferromagnetic ordering is not needed to observe the magneto-optic effect as discussed already by Brochard and de Gennes.[23] In paramagnetic suspensions the reorientation of the director can be observed when the magnetic field is applied perpendicularly to the magnetic moments of the particles. Although the idea to enhance the sensitivity of NLC to the magnetic field by adding magnetic nanoparticles is very old,[23] aggregation of the magnetic particles was the main experimental problem. As pointed out in (ref. 3) the aggregation can be prevented by nematic mediated interaction, which crucially depends on the shape of the particles and the anchoring on their surface. Perpendicular anchoring has been shown to stabilize suspensions of platelets[3] and of elongated particles.[24] While the magnetic moments of the platelets are parallel to the director, the long axis and the magnetic moments of the elongated particles lay in the plane perpendicular to the director. In (ref. 24) a small magnetic field was used to orient them in the same direction. This interesting field induced biaxial phase showed a large magneto-optic effect when the field was applied along the director, *i.e.*, perpendicular to the magnetic moments. However, the application of the field also caused reversible flocculation of the particles.

In other studies to avoid aggregation only very diluted stable suspensions of elongated ferromagnetic particles in nematic liquid crystals were experimentally realized, where magnetic interaction between the particles was negligible and, in many cases the reorientation of the nematic director was observed at lower magnetic fields compared to the field needed to reorient a pure liquid crystal.[25–29] A small low field magneto-optic response was observed in a more concentrated suspension, where in most cases the suspensions showed aggregation.[27–29] This magneto-optic response is at least two orders of magnitude weaker than the one we observed in the transverse field.

Conclusions

We have studied the response of the ferromagnetic liquid crystal to external magnetic and electric fields, and compared it to the usual response of the pure NLC. We have observed effects, which are not present in the pure NLC and are a consequence of the coupling between the nematic director and the magnetization. The electro-optic effect, which is in the ferromagnetic phase, the same as in the pure NLC, is accompanied by a converse magnetoelectric effect. The system is so a rather unique example of a soft material, in which the magnetization can be controlled by an external electric field. The magneto-optic effect differs completely from the one observed in the pure NLC, where it is a quadratic effect and it only appears when a magnetic field larger than a critical field is applied perpendicular to the director. In the ferromagnetic NLC we observe two types of magneto-optic effects. In addition to the response to the field perpendicular to the director, there is also a qualitatively different response to the parallel field. Contrary to the pure NLC no critical field needs to be exceeded for the system to respond to a field applied perpendicularly to the director, but a critical field needs to be exceeded to observe a response from the material to the field applied parallel to the director and antiparallel to magnetization. The critical field is in this case two orders of magnitude smaller than the critical field of the magnetic Frederiks transition in the pure NLC. The observed effects form the basis for the possible applications of the material.

In future work we will focus on dynamics of the response of ferromagnetic liquid crystals to external fields. While measurements of the dynamics of the director are well established, how to measure fast dynamics of small magnetization is still a challenge.

Materials and experimental methods

Sample preparation

Ferromagnetic suspension has been prepared by quenching a suspension of scandium-doped barium hexaferrite (BaHF) single crystal nanoplatelets[30] in pentylcyanobiphenyl (5CB, Nematel) from isotropic to the nematic phase.[3] The thickness of the platelets is about 5 nm; the distribution of the platelet diameter is approximately log-normal, with a mean of 70 nm and a standard deviation of 38 nm. The nanoplatelets are magnetically monodomain with magnetic moments perpendicular to the plane of the platelets. Dodecylbenzenesulphonic acid was used as a surfactant. It favours a perpendicular orientation of **n** at the surface of the particles, so the platelets in the NLC orient themselves with the surface normally parallel to **n**, *i.e.* with magnetic moments parallel to **n**. The suspension in the nematic phase was centrifuged and then the aggregated free part was filled in the LC cells (Instec, Inc.) with ITO coated and rubbed polyimide surfaces to achieve excellent planar orientation. The thickness of the cells was $d = 20.4$ μm. Initially the samples were polydomain and a strong enough magnetic field was used to transform the samples to monodomain ones. From the measured value of magnetization we estimated the volume concentration of the platelets to be 3×10^{-4}. All the measurements were performed at 25 °C.

Magnetization measurements

The magnetization curves of the samples were measured using a vibrating-sample magnetometer (LakeShore 7400 Series VSM). From the measured magnetization curves the diamagnetic contribution measured in a cell filled with pure 5CB was subtracted to obtain the magnetization curve belonging to the magnetic platelets, *i.e.*, magnetization of the sample.

Measurements of the phase difference

Changes in the director orientation in the sample were measured using polarizing microscopy. The sample was rotated between crossed polarizers so that the angle between the polarizer and the director was 45°. The intensity of monochromatic light transmitted through the sample was measured to determine the phase difference ϕ between the ordinary and extraordinary light. An interference filter with $\lambda = 632.8$ nm was used to filter the light from the halogen lamp used in the microscope. From the measurement the normalized phase difference $1 - \frac{\phi(U \text{ or } H)}{\phi(0)}$ was determined, where $\phi(0)$ is the phase difference in the zero magnetic or electric field. U is the amplitude of the AC voltage ($f = 10$ kHz) applied between the ITO electrodes.

Relation between the measurements and the model

We chose the z axis of the coordinate system to be along the undeformed director and magnetization and the x axis to be perpendicular to the cell surface, *i.e.*, in the direction of external fields. The distorted director and magnetization are only functions of x and can be represented by unit vectors, $\mathbf{n} = (\sin\varphi, 0, \cos\varphi)$ and $\mathbf{M}/M = (\sin\psi, 0, \cos\psi)$, where angles φ and ψ are functions of x. The measured magnetization and the phase difference are related to φ and ψ by

$$M_x = M\int_0^d \sin\psi(x)\mathrm{d}x \tag{8}$$

and

$$\phi = k_0\int_0^d \left(n_\mathrm{e}(x) - n_\mathrm{o}\right)\mathrm{d}x \tag{9}$$

where $n_\mathrm{e}^{-2}(x) = n_{0\mathrm{e}}^{-2}\cos^2\varphi(x) + n_\mathrm{o}^{-2}\sin^2\varphi(x)$ and $n_{0\mathrm{e}}$ and n_o are extraordinary and ordinary refractive indices, respectively. $k_0 = \frac{2\pi}{\lambda}$. From the phase difference in the absence of external fields, $\phi(0) = (n_{0\mathrm{e}} - n_\mathrm{o})k_0 d$, the anisotropy of the index of refraction $\Delta n = n_{0\mathrm{e}} - n_\mathrm{o}$ is determined.

Taking into account $\nabla \times \mathbf{E} = 0$ and $\nabla\cdot\mathbf{D} = 0$, the electric part of the free energy density can be written as

$$\frac{1}{2}\mathbf{D}\cdot\mathbf{E} = \frac{{D_x}^2}{\varepsilon_0}\frac{1}{\varepsilon_\mathrm{a}\sin^2\varphi + \varepsilon_\perp} \tag{10}$$

where D_x is a constant related to the applied voltage

$$U = \frac{D_x}{\varepsilon_0}\int_0^d \frac{\mathrm{d}x}{\varepsilon_\mathrm{a}\sin^2\varphi + \varepsilon_\perp}. \tag{11}$$

Fitting procedure

Distortion of $\mathbf{n}$ and $\mathbf{M}$ in an external field was calculated by numerical minimization of the free energy density per area, *i.e.*, eqn (1), with respect to φ and ψ. The distortions were calculated for a set of D_x or H for estimates of parameters $p = \{K_1, K_3, W, \varphi_\mathrm{s}, \gamma\}$, where φ_s is the angle describing the preferred direction of the director at the surface $\mathbf{n}_\mathrm{s} = (\sin\varphi_\mathrm{s}, 0, \cos\varphi_\mathrm{s})$. From the distortions the phase difference ϕ and the magnetization M_x were calculated as functions of U or H. The parameters that describe the experiments best were determined using a least square fitting procedure. This method is better than the usual fitting procedure[31] of Frederiks transition since it includes finite anchoring and pretilt angle φ_s.

Differential dynamic microscopy (DDM)

DDM is an alternative method to dynamic light scattering. It has been demonstrated that it can be used in bulk nematic liquid crystals to measure relaxation rates of orientational fluctuations.[21] Its advantage is that it can also probe slow dynamics at small wavevectors where usual dynamic light scattering experiments are difficult to perform. We have extended the method to also probe the confined NLCs.

We used a Nikon Eclipse Ti microscope with 10x objective (NA = 0.25). The light source of the microscope was a halogen lamp (Osram HLX64623), the numerical aperture of the condenser was set to 0.1. The polarization of the incoming light was along the z-axis, *i.e.*, it coincided with the direction of the nematic director. The analyzer was parallel to the polarizer. For each value of the magnetic field a sequence of 22 500 images with a resolution of 512 × 512 pixels and a frame rate of 50 images per second was taken with a CMOS camera (IDS Imaging UI-3370CP).

It can be shown that in such a geometry the splay-bend mode can be measured when the in-plane component of the wavevector is parallel to $\mathbf{n}$[32] and the twist mode when it is perpendicular to $\mathbf{n}$. The linear fit of the dependence of the relaxation rate on the square of the in-plane wavevector gives the relaxation rate of the fundamental splay mode in the splay-bend case, and a sum of the modes with $q_0 = \frac{\pi}{d}$ and $q_1 = \frac{2\pi}{d}$ in the twist case. The relaxation rate obtained in the latter case has for pure NLC a value between the relaxation rates of both modes, *i.e.* $\frac{1}{\tau_0} = \frac{K_2}{\gamma_1}{q_0}^2$ and $\frac{1}{\tau_1} = \frac{K_2}{\gamma_1}{q_1}^2$, where γ_1 is the rotational viscosity of the NLC.[13] In the ferromagnetic NLC the orientational fluctuations of $\mathbf{n}$ and $\mathbf{M}$ are coupled and, consequently, the relaxation rates are more complicated,[3] but still have a similar wavevector dependence.

Acknowledgements

The authors acknowledge the support from Slovenian Research Agency (A. M., N. O. and, M. Č. grant no. P1-0192; D. L. grant no. P2-0089-4). We thank the CENN Nanocenter for use of the LakeShore 7400 Series VSM vibrating-sample magnetometer.

References

1 D. N. Paulson and J. C. Wheatley, *Phys. Rev. Lett.*, 1978, **40**, 557–561.
2 T. Albrecht, C. Bührer, M. Fähnle, K. Maier, D. Platzek and J. Reske, *Appl. Phys. A: Mater. Sci. Process.*, 1997, **65**, 215–220.
3 A. Mertelj, D. Lisjak, M. Drofenik and M. Čopič, *Nature*, 2013, **504**, 237–241.

4 J. W. Goodby, *Ferroelectric Liquid Crystals: Principles, Properties and Applications*, Gordon and Breach Science Publishers, 1991.
5 T. Niori, T. Sekine, J. Watanabe, T. Furukawa and H. Takezoe, *J. Mater. Chem.*, 1996, **6**, 1231–1233.
6 H. Bock and W. Helfrich, *Liq. Cryst.*, 1992, **12**, 697–703.
7 K. Kishikawa, S. Nakahara, Y. Nishikawa, S. Kohmoto and M. Yamamoto, *J. Am. Chem. Soc.*, 2005, **127**, 2565–2571.
8 V. Wadhawan, *Introduction to Ferroic Materials*, CRC Press, 2000.
9 N. A. Spaldin and M. Fiebig, *Science*, 2005, **309**, 391–392.
10 W. Eerenstein, N. D. Mathur and J. F. Scott, *Nature*, 2006, **442**, 759–765.
11 C.-W. Nan, M. I. Bichurin, S. Dong, D. Viehland and G. Srinivasan, *J. Appl. Phys.*, 2008, **103**, 031101.
12 K. F. Wang, J.-M. Liu and Z. F. Ren, *Adv. Phys.*, 2009, **58**, 321–448.
13 P. G. de Gennes and J. Prost, *The Physics of Liquid Crystals*, Clarendon Press, 2nd edn, 1995.
14 P. M. Chaikin and T. C. Lubensky, *Principles of Condensed Matter Physics*, Cambridge University Press, Reprint, 2000.
15 A. I. Liechtenstein, M. I. Katsnelson and V. A. Gubanov, *J. Phys. F: Met. Phys.*, 1984, **14**, L125–L128.
16 P. Galatola, C. Oldano and M. Rajteri, *Phys. Rev. E: Stat. Phys., Plasmas, Fluids, Relat. Interdiscip. Top.*, 1994, **49**, 1458–1467.
17 P. Galatola and M. Rajteri, *Phys. Rev. E: Stat. Phys., Plasmas, Fluids, Relat. Interdiscip. Top.*, 1994, **49**, 623–628.
18 K. Eidner, M. Lewis, H. K. M. Vithana and D. L. Johnson, *Phys. Rev. A: At., Mol., Opt. Phys.*, 1989, **40**, 6388–6394.
19 I. D. Olenik, M. Jazbinšek and M. Čopič, *Phys. Rev. Lett.*, 1999, **82**, 2103–2106.
20 R. Cerbino and V. Trappe, *Phys. Rev. Lett.*, 2008, **100**, 188102.
21 F. Giavazzi, S. Crotti, A. Speciale, F. Serra, G. Zanchetta, V. Trappe, M. Buscaglia, T. Bellini and R. Cerbino, *Soft Matter*, 2014, **10**, 3938–3949.
22 S. V. Burylov and Y. L. Raikher, *Mol. Cryst. Liq. Cryst. Sci. Technol., Sect. A*, 1995, **258**, 107–122.
23 F. Brochard and P. G. de Gennes, *J. Phys.*, 1970, **31**, 691–708.
24 S.-H. Chen and N. M. Amer, *Phys. Rev. Lett.*, 1983, **51**, 2298–2301.
25 P. Kopčanský, N. Tomašovičová, M. Koneracká, V. Závišová, M. Timko, A. Džarová, A. Šprincová, N. Éber, K. Fodor-Csorba, T. Tóth-Katona, A. Vajda and J. Jadzyn, *Phys. Rev. E: Stat., Nonlinear, Soft Matter Phys.*, 2008, **78**, 011702.
26 E. Ouskova, O. Buluy, C. Blanc, H. Dietsch and A. Mertelj, *Mol. Cryst. Liq. Cryst.*, 2010, **525**, 104–111.
27 N. Podoliak, O. Buchnev, O. Buluy, G. D'Alessandro, M. Kaczmarek, Y. Reznikov and T. J. Sluckin, *Soft Matter*, 2011, **7**, 4742–4749.
28 O. Buluy, S. Nepijko, V. Reshetnyak, E. Ouskova, V. Zadorozhnii, A. Leonhardt, M. Ritschel, G. Schönhense and Y. Reznikov, *Soft Matter*, 2011, **7**, 644–649.
29 N. Tomašovičová, M. Timko, Z. Mitróová, M. Koneracká, M. Rajňak, N. Éber, T. Tóth-Katona, X. Chaud, J. Jadzyn and P. Kopčanský, *Phys. Rev. E: Stat., Nonlinear, Soft Matter Phys.*, 2013, **87**, 014501.
30 D. Lisjak and M. Drofenik, *Cryst. Growth Des.*, 2012, **12**, 5174–5179.
31 S. W. Morris, P. Palffy-Muhoray and D. A. Balzarini, *Mol. Cryst. Liq. Cryst.*, 1986, **139**, 263–280.
32 M. Čopič, M. Vilfan and A. Mertelj, *Liq. Cryst.*, 2013, **40**, 1646–1654.

